

Contents listsavailable at ScienceDirect

Neurotherapeutics

journal homepage: www.sciencedirect.com/journal/neurotherapeutics



Original Article

AAV6 mediated Gsxl expression in neural stem progenitor cells promotes neurogenesis and restores locomotor function after contusion spinal cord injury

Zachary Finkela, Fatima Estebana, Brianna Rodrigueza, Tanner Clifforda, Adelina Josepha, Hani Alostaz 3, Mridul Dalmia 3, Juan Gutierreza, h, Matthew J. Tamasia, Samuel Ming Zhanga, Jonah Simonea, Hafize Petekci 3, Susmita Natha, Miriam Escotta, Shivam Kumar Garga, Adam J. Gormley 3, Suneel Kumar 3, Sonia Gulati C, Li Caia, c, *

- Dq,anmmt of Bi<>medkal EngineaiJl& Rutgm UniYersily, 59'}Tqylor Rd, Piscataway, NJ 08854, USA
- ь University of califom.a, samn Barbara, CA 93106, USA
- c NeuroNovu.s Therapeutics Inc., 135 E 57thSt, New Y<rk, NY 10022, USA

ARTICLE INFO

Keywords: Genomic screened homeobox 1 (Gshl or Gsxl) Geoe therapy Neural stem/progenitor cell Neurogenesis Neural regeocration Traumatic spinal rord injury

ABSTRACT

Genomic screened homeobox 1 (Gsxl or Gshl) is a neurogenic transcription factor required for the generation of excitatory and inhibitory interneurons during spinal cord development. In the adult, lentivirus (LV) mediated Gsxl expression promotes neural regeneration and functional locomotor rerove,y in a mouse model of lateral hemisection spinal cord injury (SQ). The LV delivery method is clinically unsafe due to insertional mutations to the host DNA. In addition, the most common clinical case of SCI is contusion/compression. In this study, we identify that adeno-associated virusserotype 6 (AAV6) preferentially infects neural stem/progenitorcells (NSPCs) in the injured spinal rord. Using a rat model of contusion SCI, we demonstrate that AAV6 mediated Gsxl expression promotes neurogenesis, increases the number of neuroblasts/immature neurons, restores excitatory/inhibitory neuron balance and serotonergic neuronal activity through the lesion rore, and promotes locomotor functional rerove,y. Our findings support that AAV6 preferentially targets NSI'a forgene deliveryand ronfinned Gsxl efficacy in clinically relevant rat model of contusion SCI.

Introduction

Spinal cord injury (SCI) is a complex tissue injury resulting in degenerating damage to the central nervous system (CNS) and is characterized by low quality of life. The clinical pathophysiology of SCI is heterogenous and greatly affected by the extent, location, and type of injury [1]. Immediately following initial mechanical damage, a cascade of cellular/molecular effects occurs, resulting in localization of inflammatory cells to the injury site [2], mass cell apoptosis [3], release of reactive oxygen species [4], and glutamate-mduced excitotoxicity[5]. Dernyelination and neuronal degeneration occur in the mechanically damaged and adjacent spared tissue. The resulting microenvironment is unfavorable for cellular growth and isolated by the glial scar border over a period of weeks.

Neural stem/progenitorcells (NSPCs), characteriz.edby multipotency and self-renewal, are highly diver..e with various established marker..,

e.g., Nestin, Sox2, Foxjl, and NG2 [6--8]. These unique cells produce newborn neurons and glia in the neurogenic niches of the developing and adult CNS [9]. In the normal adultspinal cord, NSPCs are quiescent; they become activated and proliferate to contribute glial fated progeny to the glial scar after injury [10]. NSPCs are a major target for regenerative therapy to treat SCI (see reviews in Refs. [7,11]).

The genomic screened homeobox 1 (Gsxl or Gshl) is a neurogenic transcription factor known to regulate the formation ofdorsal excitatory and inhibitory spinal cord interneurons during embryonic development [12,13]. In the adult, the roleofinhibitory dorsal interneuron population four is to modulate our perception of pain and itch sensation, whereas excitatory dorsal population five modulates our perception of pain, itch, heat, and touch sensation [14]. Interestingly, the mature dorsal populations formed via Gsxl expression in the embryo do not contribute to circuits involved in motor function. However, our recent study

E-mail address: lcai@rutgers.edu (L. Cai).

^{*} Corresponding author.

demonstrated that lentivirus (LV) mediated Gsxl (LV-Gsxl) expression largely affects NSPCs, reduces reactive gliosis and glial scar formation, promotes serotonin (5-HT) neuronal activity and locomotor functional recovery in a mouse model oflateral hemisection SCI [15]. In addition, virus mediated Sox2 expression directlyconverts GFAP+ astrocytes [16] and NG2+ polydendrocytes [17] into neurons, and results in functional improvement in a mouse model of hemisection SCI.

While it has been demonstrated that Gsxl, Sox2, and other neurogenic factors promote regeneration after SCI [16--19], the LV gene delivery method is notideal. As a retrovirus, the LV incorporates its genome into the host DNA and is proneto random insertional mutations [20]. The adeno-associated virus (AAV) is a clinically safe alternative as its mechanism of action does not require incorporation of its genome into the host DNA, and thus reduces risk of harm to the patient [21]. A cell specific promoter, e.g., GFAP for astrocytes and NG2 for polydendrocytes, or a particular AAV serotype can be used to target various cellpopulations in the spinal cord.

Thegoalof the Gsxl therapeutic is to targetand engineer endogenous NSPCs to producefunctional interneurons instead of glia to restore signal transmission through the injury site. In this study, we first identify that AAV serotype 6 (AAV6) is a highly effective gene delivery system to target NSPCsin the injuredspinal cord. We then examine the efficacy of both AAV6-Gsxl and LV-Gsxl in a clinically relevant rat model of contusion SCI. Overall, our study advances the development of clinically relevant AAV6-based gene therapy for NSPC targeting and provides insight into the cellular/molecular and behavioral effects of Gsxl reactivation in adult rat models of SQ.

Results

AAV6 preferentially transduces NSPCs in the injured rat spinal rord

Since LV bears biosafety concerns, e.g., insertional mutagenesis [22-24], we performed a literaturesearch for AAV serotypes with NSPC affinity. Initially, we identified three potential serotypes: AAV5 [25,26], AAV6 [25,27], and AAVrhlO [28,29] based on their known tropism. We then evaluated which AAV serotype transduces NSPCs with the highest efficiency. We screened the three selected candidates in a rat model of lateral hemisection SQ. Viral constructs with a ubiquitous cytomegalovirus (CMV) promoter and GFP reporter, i.e., AAV5-GFP, AAV6-GFP, and AAVrlllO-GFP, were selected and tested. LV-GFP served as a positive control. A total number of 12 male Sprague Dawley rats were randomly divided into the following groups: SQ+ AAV5-GFP, SQ+ AAV6-GFP, SQ + AAVrhl0-GFP, SQ + LV-GFP. A total of 3.0 µl virus was injected at three depths into the spinal cord at 500 nl/min: 0.5 mm, 1.0 mm, 1.5 mm, at approximately 1.0 mm rostral/caudal to the injury site immediatelyfollowing SQ (supplemental Fig. SI). Animals were sacrificed and spinal cords were harvested in the acute stage at 4 days post-injury (4 dpi) (supplemental Fig. SI).

Immunohistochemistry OHC) analysis was performed to quantify the expression of well-established NSPC marker Nestin. The efficiency of viral transduction was determined by the percentage of virally infected cells (GFP+) among the total number of cells (DAPI+) at the viral injectionsite adjacent to the lesion core (Fig. 1). Transduction efficiency in NSPCs was defined as the percentage of GFP and Nestin co-labeled cells (GFP+/Nestin+) among virallyinfected cells (GFP+). We observed that the GFP+ cells were concentrated at the injection sites and evenly distributed throughout the injury, approximately 1 mm rostral/caudalto the lesion core (supplemental Fig. S2). The Nestin+ cells were concentrated near the lesion site and did not distinctly pass through the ependymal layer of the central canal (CC) into the uninjured side. However, some NSPC activation was observed on the uninjured lateral side closest to the hemisection injury (Fig. la).

Cell count analysis showed the percentage of AAV6-GFP+ cells (85.36% \pm 0.52; n= 3) andAAVrlllO-GFP+cells (87.32% \pm 0.95; n= 3) among the total number of cells (DAPI+) in the counted area were

significantly higher than that of the AAV5-GFP group (76.20% \pm 1.53; n = 3), compared with the percentage of LV-GFP (83.75% \pm 3.40; n = 3) control group. This indicates that the serotypes of AAV6 and AAVrhlO have a higher transduction efficiency than AAV5 (Fig. 1b). The percentage of GFP+/Nestin+ cells among virally infected cells (GFP+) in AAV6-GFP (71.75% \pm 2.28; n = 3)and AAVrlllO-GFP (58.84% \pm 4.59;n = 3) were significantly higher than that of AAV5-GFP group (44.71% \pm 3.07; n = 3), compared with LV-GFP (72.89% \pm 8.75; n = 3) control (Fig. le). While no significant difference in transduced NSPCs was found between AAV6-GFP and AAVrhlO-GFP, a trend and greater significant difference with AAV5-GFP infected NSPCs (Fig. lb) indicates that AAV6 serotype has the highest transduction efficiency for NSPCs. The high transduction efficiency and NSPC specific transduction rates reflect the infected cells at the injection sites, directly overlapping with a region of high NSPC activation after SQ. Based on our findings, the NSPC specific AAV6wasselected to further test the efficacy of Gsxl forSQ treatment in a rat model of contusion SCI.

AAV6-Gsxl promotes NSPC activation, proliferation, and neurogen.esis in the acute SCI

We next tested the efficacy of AAV6-Gsxl to activate NSPCs and induce cell proliferation in the following groups: SQ+ AAV6-GFP, SQ + AAV6-Gsxl, SCI+ LV-GFP, SQ+ LV-Gsxl-GFP in a rat model of lateral hemisection SCI (Fig. 2). We sacrificed animals and harvested spinal cordsat 4 dpi.IHCanalysis was used to quantify the expression ofNestin (NSPCs) and PCNA (proliferating cells). We found co-labeled Nestin+/ GFP+ cells throughout and immediately adjacent to the lateral hemisection injury site and expressed this value among virally infected cells (GFP+) to represent the virus induced NSPC activation (Fig. 2a). Wealso expressed this value as a percentage of total cells (DAPI+) and raw cell values (supplemental Fig. S3).

Cell count analysis showed that AAV6-Gsxl (39.98% \pm 4.45; n = 3) and LV-Gsxl-GFP (31.%% \pm 0.%; n = 3) significantlyincreased Nestin+ NSPC activation in comparison with controls: LV-GFP (25.45% \pm 4.32; n = 3) and AAV6-GFP (19.36% \pm 3.36; n = 3) (Fig. 2b). We also found many co-labeled PCNA+/GFP+ cells throughout the tissue surrounding the injury and injection sites (Fig. 2a) and expressed this value among virally infected cells (GFP+) to quantify virus-induced proliferation. We found that AAV6-Gsxl (33.49% \pm 3.79; n = 3) and LV-Gsxl-GFP $(28.71\% \pm 6.91; n = 3)$ significantly increased cell proliferation in comparison with controls LV-GFP (10.86% \pm 2.94; n = 3) and AAV6-GFP $(15.74\% \pm 1.97; n = 3)$ (Fig. 2c). We further investigated Gsxl-induced neurogenesis by quantifying cells with the co-labelingof markers: virally infected (GFP+) proliferating (PCNA+) NSPCs (Nestin+). We observed many Gsxl-induced co-labeled neurogenesis positive cells between the 1 mm rostral/caudal of the injection sites and throughout the injury (Fig. 2a). AAV6-Gsxl $(18.300/4 \pm 2.80; n = 3)$ and LV-Gsxl-GFP (13.66%± 2.93; n = 3) induced neurogenesis in comparison with controls LV-GFP $(3.84\% \pm 1.28; n = 3)$ and AAV6-GFP $(2.97\% \pm 0.95; n = 3)$ (Fig. 2d), e.g., AAV6-Gsxl-induced activated proliferating NSPCs (Fig. 2e). We found that Gsxl promoted NSPC activation and proliferation, and induced neurogenesis in the acute injured spinal cord.

We proceeded to investigate AAV6-Gsxl-induced NSPC activation, proliferation, and neurogenesis in a moreclinically relevant rat model of contusion SCI (Fig. 2). Rats were subject to contusion SCI and injected with viral treatments in the following groups: SQ + AAV6-GFP, SQ + AAV6-Gsxl, SQ+ LV-Gsxl-GFP. A total of3.0 µl virus was injected into the spinal cord in four comers of the contusion injurysiteapproximately 1 mm rostral/caudal to the epicenter immediately following SQ (supplemental Fig. SI). The consistency of each contusion injury was confirmed visually during surgery and behaviorally following surgery with complete rear hind limb paralysis below the thoracic injury level. We sacrificed animals and harvested spinal cords at 4 dpi. IHC analysis was used to quantify the expression of Nestin (NSPCs), Sox2 (neural progenitor cells), NG2 (glial progenitor cells/polydendrocytes), and

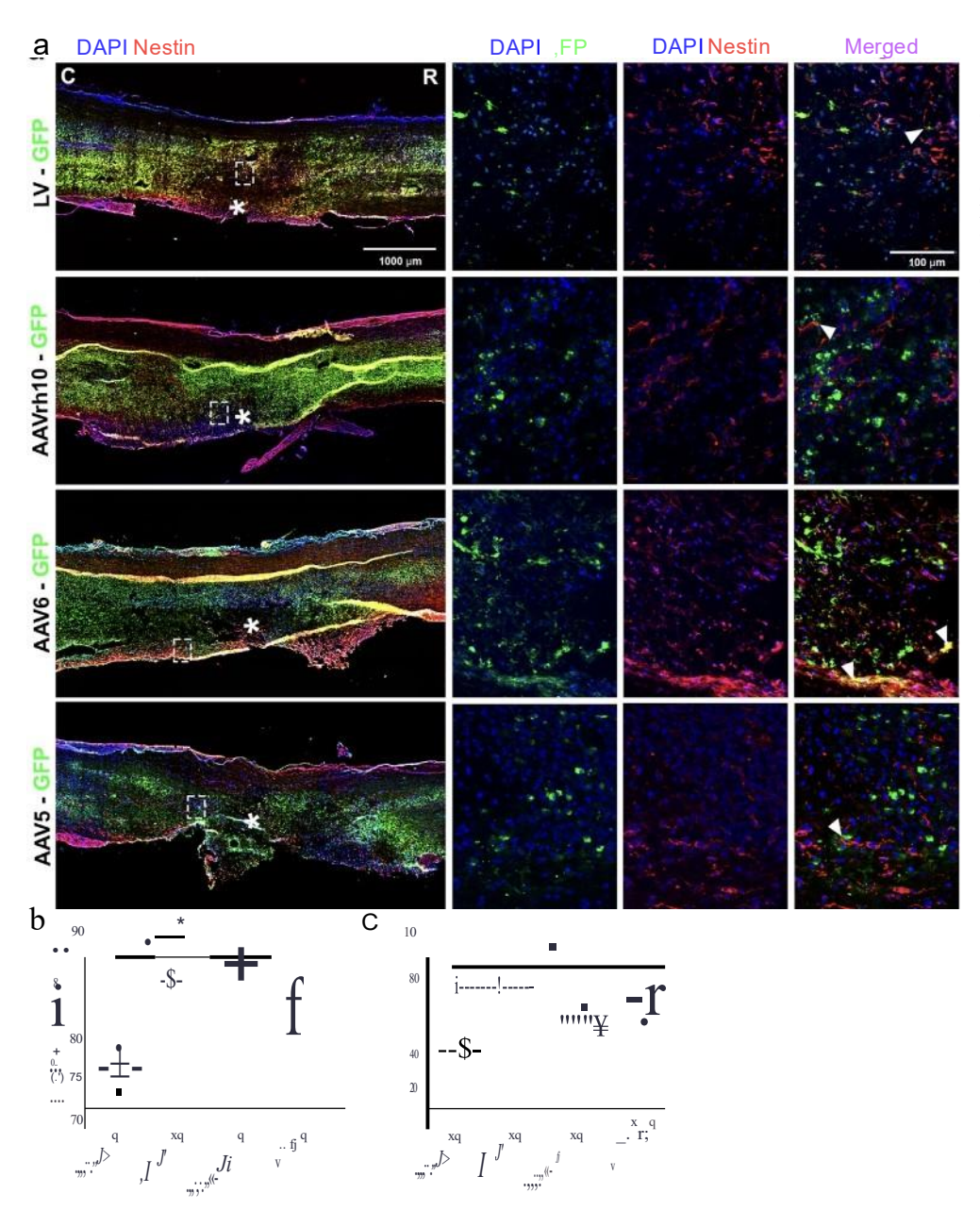


Fig. 1. AAV serotype 6 targets NSPCs in acute SCI. (a) Representative immunofluorescence photomicrograph of virally transduced cells (green) and NSPCs (Nestin, red) in longitudinal spinal cord sections at 4 dpi. (b) Pen:entage of GFP+ cells over DAPI+ cells adjacent to the lesion epicenter. (c) Percentage of GFP+Nestin+ cells over total GFP+ cells adjacent to the lesion epicenter. Data are expressed as mean ± SFM. *p < 0.05, AAVS-GFP, AAV6-GFP, and AAVrhlO-GFP versus the oontrol group (LV-GFP). Statistical analysis was performed using a one-way ANOVA followed by Tukey's post hoc test

PCNA (proliferating cells). The virally infected GFP+ cell signal was distributed evenlyoneithersideof thecontusion injurysite, sparse in the lesion core, and consistently dispersed throughout the lesion border (supplemental Fig. S4). The majority of GFP+ cells were found at/near lesion or injection site and appeared to diffuse in the rostral/caudal directions. The Nestinsignal was prominent in the lesion borderand spread rostral/caudal neural tissue. Nestin+/GFP+ and PCNA+/GFP+ colabeled cells among total cells (DAPI+) (Fig. 20 and virally infected cells (GFP+) (supplemental Fig. S5) were quantified.

Cell count analysis showed that AAV6-Gsxl (5.04% ± 0.02; n = 3) and LV-Gsxl-GFP (7.35% ± 0.51; n = 3) increase Nestin+ NSPC activation in comparison to control (3.18% ± 0.77; n = 3) (Fig. 2g). The PCNAsignal wasless obviousbut overlapped with the Nestin throughout the lesion border (Fig. 2f). We found thatAAV6-Gsxl (12.01% ± 0.8; n = 3) and LV-Gsxl-GFP (13.29% ± 2.18;n = 3) did notsignificantly increase cell proliferation in comparison with the control (7.72% ± 1.41; n = 3), however a positive trend is obvious (supplemental Fig. S5). To investigate neurogenesis in the NSPC populations, we observed and quantified the co-labeling of GFP+, Nestin+, and PCNA+ cells in the injured spinal

cord (Fig. 2h). We found that AAV6-Gsxl $(8.09\% \pm 0.83; n = 3)$ and LV-Gsxl-GFP $(8.38\% \pm 0.63; n = 3)$ induce neurogenesis in comparison to control $(3.68\% \pm 0.98; n = 3)$ (Fig. 2h), e.g., a group of AAV6-Gsxl-induced proliferating NSPCs between the lesion core and caudal injection site (Fig. 2i).

We alsoobserved activation of NG2+ progenitors approximately 1.5 mm rostral/caudal to the injury site, counted co-labeled NG2+/GFP+cells, and expressed over the GFP+ population (supplemental Fig. S6a). We found that AAV6-Gsxl (8.26% \pm 2.07; n = 3) and LV-Gsxl-GFP (8.100/4 \pm 2.11; n = 3) do not significantly increase NG2+ NSPC activation in comparison to the control (10.01% \pm 2.16; n = 3) (supplemental Fig. S6c). In addition, we observed Sox2 neural progenitor activation throughout the lesion site and counted co-labeled Sox2+/GFP+ cells and expressed over the GFP+ population (supplemental Fig.S7a). We found that AAV6-Gsxl (48.85% \pm 2.61; n =3) significantly increased Sox2+ NSPC activation in comparison with the control (29.51% \pm 1.74; n = 3) (supplemental Fig. S7c). However, LV-Gsxl-GFP (37.21% \pm 4.73; n = 3) did not significantly activate Sox2 progenitors (supplemental Fig. S7c).

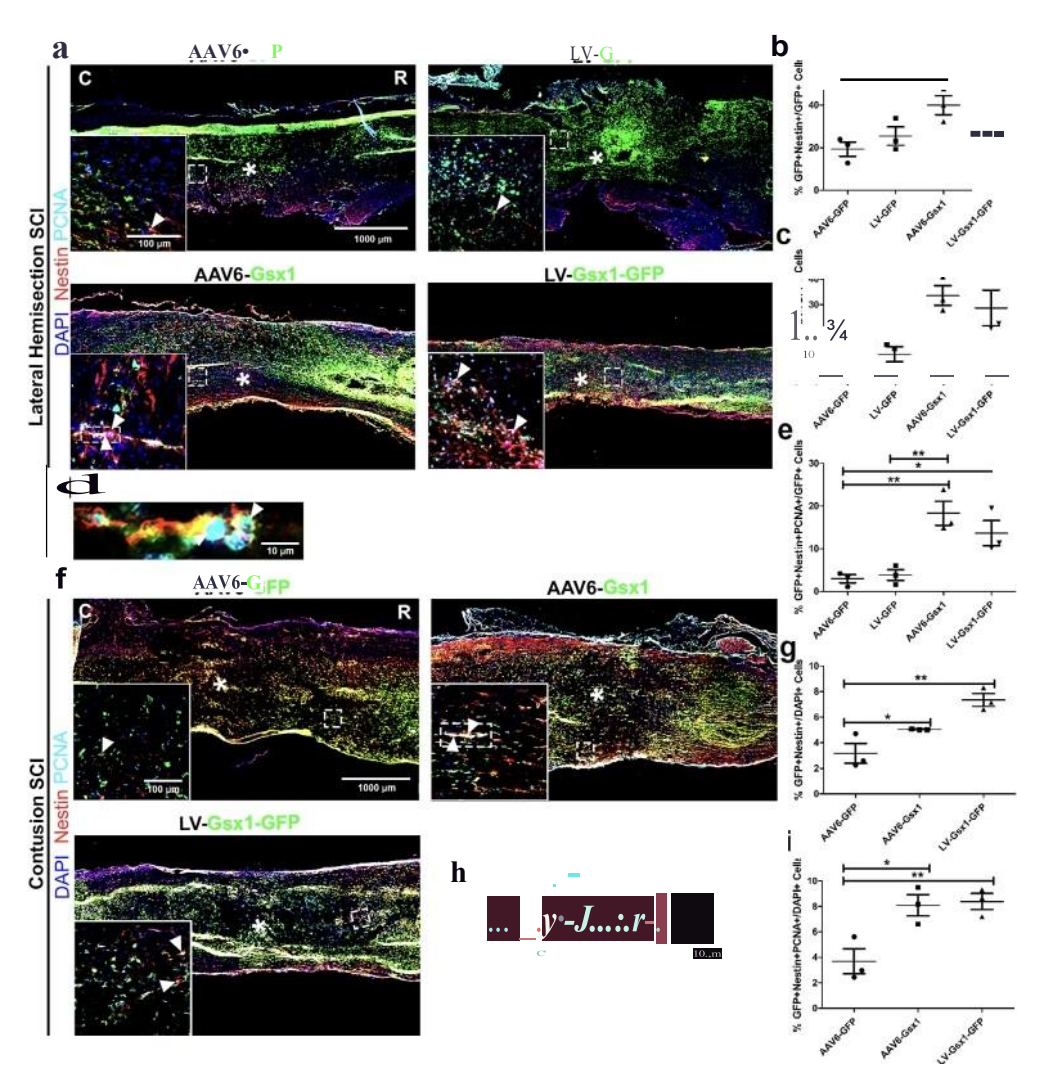


Fig. 2. Gsx1 promotes NSPC activation, proliferation, and neurogenesis in acute heinisection and contusion SCI. Representative imm\lllofluorescence photomicrograph of virally transduced cells (green), NSPCs (Nestin, red), and proliferation (PCNA, cyan) in longitudinal spinal cord sections at 4 dpi. (b) Percentage of GFP+Nestin+ cells over total GFP+ cells adjacent to the lesion epicenter. (c) Percentage of GFP+PCNA+ cells over total GFP+ cells adjacent to the lesion epicenter. (d) Percentage of Nestin+PCNA+GFP+ cells over total GFP+ cells adjacent to the lesion epicenter. (e) Representative imrnllllofluorescence photomicrograph of virally infected (Gsxl+) proliferating (PCNA+) neural stem cells (Nestin+) in the injured spinal rord with AAV6-Gsxl treatment. (0 Representative immllllofluorescence photomicrogra)il of virally transduced cells (in green), NSPCs (Nestin, red), and proliferation (PCNA, cyan) in longitudinal spinal rord sections at 4 dpi. (g) Percentage of GFP+Nestin+ cells over total DAPI+ cells at injection sites adjacent to the lesion epicenter. (h) Representative immllllofluorescence photomicrograph of virally infected (Gsxl+) proliferating (PCNA+) neural stem cells (Nestin+) in the injured spinal cord with AAV6-Gsxl treatment. (i) Percentage of Nestin+PCNA+GFP+ cells over total DAPI+ cells adjacent to the lesion epicenter. AAV6-Gsxl and LV-Gsxl induce neurogenesis in the injured spinal cord. Data are expressed as mean± SEM.*p <0.05, **p < 0.01, AAV6-Gsxl and LV-Gsxl-GFP versus the rontrol groups (AAV6-GFP, LV-OFP). Statistical analysis was peiformed using a one-way ANOVA followed by Tukey's post hoc test.

We used llastik [30], a non-biased machine learning based bioimage pixel classification analysis software to supplement our cell count analysis and quantified the total molecular marker signal among total cells. We found no difference in transduction efficiency between AAV6-Gsxl $(6.37\% \pm 0.34; n = 3)$, LV-Gsxl-GFP $(8.02\% \pm 1.27; n = 3)$, and control AAV6-GFP (5.18% \pm 0.52; n = 3) (supplemental Fig. S8a). AAV6-Gsxl $(4.29\% \pm 0.34; n = 3)$ and LV-Gsxl-GFP $(4.35\% \pm 0.24; n = 3)$ 3) promoted Nestin+ NSPC activation in comparison to control (2.300/4 \pm 0.21; n = 3) (supplemental Fig. S9a). AAV6-Gsxl (1.31% \pm 0.08; n = 3) and LV-Gsxl-GFP (1.28% \pm 0.14; n = 3) increased cell proliferation in comparison with the control (0.75\% \pm 0.04; n = 3) (supplemental Fig. S9b). We investigated total NG2 progenitor activation and found that AAV6-Gsxl (12.91% \pm 0.57; n = 3) activated NG2 polydendrocytes in comparison with the control (8.88% \pm 0.69; n = 3) (supplemental Fig. S6c). Interestingly, LV-Gsxl-GFP did not activate NG2 polydendrocytes in comparison with the control (supplemental Fig. S6b). We investigated total Sox2 progenitor activation and found that AAV6-Gsxl $(1.98\% \pm 0.18; n = 3)$ and LV-Gsxl-GFP $(2.26\% \pm 0.21; n = 3)$ did not activate Sox2+ neural progenitors in comparison with the control $(2.23\% \pm 0.28; n = 3)$ (supplemental Fig. S7b).

Overall, Gsxl activated various NSPC populations, increased cell proliferation, and induced neurogenesis in both the rat models of lateral hemisection and contusion SCI. The contusion SQ model is representative of the most common clinical injury and is thus used for our Gsxl therapy efficacy analysis in three major stages: acute, subacute, and chronic.

AAV6-Gsxl promo/ES neuroblast and immarure neuron formation in the subacute contusion SCI

We next examined the presence of newborn or immature neuron formation at 14 dpi (subacute SCI) initiated by Gsxl-induced neurogenesis at 4 dpi (Supplemental Fig. SI). Rats were subject to contusion SQ and injected with viral treatments in the following three groups: SQ + AAV6-GFP, SCI+ AAV6-Gsxl, SQ + LV-Gsxl-GFP. A total of 3.0 μl virus was injected into the spinal cord in four comers of the contusion injury site approximately 1 mm rostraVcaudal to the epicenter immediately following SQ. Animals were sacrificed and spinal cords were harvested at 14 dpi.

IHC analysis was used to examine the injured spinal cord for established molecular markers DCX (neuroblasts), Tujl (immature neurons), and Notchl (canonical notch activity). The injured area was clear and tissue damage was extensive, spanning 1-2 mm rostral/caudal to the injuryepicenter (Supplemental Fig.Sl0). TheGFP+ celldistribution was concentrated at the injection sites and spread approximately 2 mm rostral/caudal to the lesioncore. GFP+ cells were clearly present rostral/caudal to the injury epicenter, throughout the injured tissue (Supplemental Fig. Sl0). We found that LV-Gsxl-GFP (10.97% \pm 0.64; n = 3) transduced a higher percentage of cells in comparison to AAV6-Gsxl (6.53% \pm 0.44; n = 3), and control AAV6-GFP (6.67% \pm 1.14; n = 3) (supplemental Fig. S8b). Tujl signal was distributed throughout the injection sites and rostral/caudal to the lesion core (Fig. 3a). We found that

AAV6-Gsxl (14.41% \pm 1.96; n = 3) significantly increased the percentage of Tujl+ cells among total cells and LV-Gsxl-GFP (10.62% ± 1.89; n = 3) did not in comparison to AAV6-GFP control (6.76% \pm 0.91; n = 3) (Fig. 3b). The canonical notch pathway is upregulated during cell proliferation and NSPC activation in early stages after SO and decreases during celldifferentiation. Here, we used the NotchI marker to support Gsxl induced differentiation, indicated by a lack of canonical pathway notch activity at 14 dpi. Our Notchl signal was evenly distributed throughout the lesion border and spared tissue 0.5 mm rostral/caudal to the injection sites (Fig. 3a). We found that LV-Gsxl-GFP (0.700/4 \pm 0.14; n = 3) significantly reduced the percentage of Notchl+ cells among total cells in comparison with the AAV6-Gsxl treatment (2.42% \pm 0.32; n = 3), supporting neuronal differentiation of LY-mediated Gsxl activated NSPCsduringsubacute SO (Fig. 3c). The DCXsignal was only present at the injection sites and dissipated into the lesion core in our control SCI group (Fig. 3d). LV-Gsxl-GFP (4.73% \pm 0.33; n = 3) significantly increased the percentage of DCX+ cells over total cells, however AAV6-Gsxl (3.36% \pm 0.12; n = 3) did not in comparison to AAV6-GFP control $(2.75 \pm 0.16; n = 3)$ (Fig. 3e).

The low percentages of newborn and immature neurons reflect the quantification area, approximately 2 mm rostral/caudal to and throughout the lesioncore, and the extentof tissue damage. Collectively, the Gsxl gene treatments promoted newborn and immature neuronal formation at 14 dpi following Gsxl-induced activation, proliferation, and neurogenesis of NSPCs at 4 dpi.

AAV6-Gsxl increases excitatory and reduces inhibitory intemeuron populations in the chronic contusion SCI

The synaptic excitatory/inhibitory cell balance in the spinal cord is maintained by intemeuron subtypes and required to functionally transmit signal from the brain through the spinal cord [31]. The neurogenic gene Gsxl drives the formation of dorsal excitatory and inhibitory interneurons during development [32]. We demonstrated that Gsxl-induced newborn and immature neurons were generated in subacute SO (Fig. 3). We next investigate the role of Gsxl on the neuronal balance and the identity of differentiated newborn and immature neurons as they develop and integrate into spinal cord neuronal circuitry. Injured animals with viral treatments were sacrificed at 56 dpi (chronicSCI)(Supplemental Fig. SI).

rnc analysis was used to examine the markers of vGlut2 (excitatory), GABA (inhibitory), and ChAT (cholinergic) interneurons. The injured area is clear and spans 2 mm rostral/caudal to the injury epicenter. The GFP+ cell distribution is concentrated at the injection sites, approximately 1-2 mm rostral/caudal to the lesion core, and some GFP+ cells can be found even further, indicating extensive viral spread. GFP+ cells were dearly present rostral/caudal to the injury epicenter, throughout the injured tissue (Supplemental Fig. Sl 1). However, no GFP+ cells were present in the injury epicenter, consistent with our findings at 4 dpi (Supplemental Fig. S4) and 14 dpi (Supplemental Fig. S9). At the injury epicenter, the microenvironment is not favorable for cell growth, thus cells do not usually survive (Supplemental Fig. S11). The vGlut2 signal was distributed throughout our control treatment rostral and slightly caudal to the injured area. Interestingly, our treatments contained many co-labeled GFP+vGlut2+ cells throughout the lesion sitespanning 4 mm rostral to caudal, indicated by yellow signal (Fig. 4a). AAV6-Gsxl (1.23% \pm 0.05; n = 3) and LV-Gsxl-GFP (1.16% \pm 0.03; n = 3) increased the percentage of VGlut2+ among total cells in comparison to controlAAV6-GFP (0.94% \pm 0.04; n = 3) (Fig. 4b). The most prominent GABA signal was present in our control and consistent rostral/caudal to the lesion core, but not present in the lesion core. We found very few if any co-labeled GFP+/GABA+ cells (Fig. 4c). AAV6-Gsxl (2.1% ± 0.22; n = 3) and LV-Gsxl-GFP (2.25% \pm 0.16; n = 3) reduced the percentage of GABA+ cellsamong total cells in comparison to control (3.62% \pm 0.12; n = 3) (Fig. 4d). The ChAT signal was distributed evenly throughout the rostral spinal cord but interrupted by the lesion site and not present caudal to the lesion (Fig. 4c). Notably, AAV6-Gsxl ($0.87\% \pm 0.19$; n = 3)

and LV-Gsxl -GFP (0.66% \pm 0.10; n = 3) did not increase ChAT+ cells in comparison to AAV6-GFP control (1.17% \pm 0.24; n = 3) (Fig. 4e).

Overall, Gsxl alters the excitatory/inhibitory cell balance in the chronic injured spinal cord by reducing inhibition and increasing excitation at the lesion core. The large number of co-labeled virally infected excitatory interneurons in our AAV6-Gsxl and LV-Gsxl-GFP treatments suggest that the newborn and immature neurons formed at 14 dpi (Fig. 3) have differentiated intoexcitatory interneurons at 56 dpi (Fig. 4).

AAV6-Gsxl reduces reactive gliosis and glial scar formati.onin the subacute and chronic SCI

The glialscar presents a physical and chemical banier toregeneration due to a dense astrocyte/fibroblast cell layer, thick secreted ECM, and inhibitory molecules, e.g., CSPGs, collogen [33]. NSPCs play a significant role in scar border formation and contribute glial fate progeny to the astrocyte scar populations [34]. Gsxl promotes newborn and immature neuronal populations in subacute SCI (Fig. 3). We also identified that these populations differentiate into excitatory and not inhibitory intemeurons (Fig. 4).

We next investigated the effect of Gsxl on reactive gliosis and glial scar formation at 14 dpi and 56 dpi. FRC analysis was used to determine the expression of GFAP (reactive astrocytes) at 14 dpi and CS56 (CSPGs) and GFAP (astrocyte density) in the mature glialscarat 56 dpi. The GFAP signal distribution at 14 dpi was most prominent in the spared neural tissue adjacent to the lesion site, and clearly astrocytes were elongating processes to begin formation of the glial scar (Fig. Sa). We found that AAV6-Gsxl (18.32% \pm 2.22; n = 3) reduced reactive gliosis (GFAP/total cells) in comparison to AAV6-GFP control (36.79% \pm 2.56; n = 3) at 14 dpi (Fig. Sb). The CS56signal distribution at 56 dpi was diffuse and most densely occurring at the scar border at the edge of the lesion core but spread 2 mm rostral/caudal to the injury site (Fig. Sc). AAV6-Gsxl $(1.48\% \pm 0.23; n = 3)$ reduced CSPG deposition (CS56/total cells) in comparison to AAV6-GFP control (3.400/o \pm 0.69; n = 3) at 56 dpi (Fig. 5d). The GFAP distribution formed a deardense bordersurrounding the injury site with diffuse signal spreading 0.5-1 mm away from the injury scar border (Fig. Se). AAV6-Gsxl (7.91% \pm 2.73; n = 3) also reduced glial scar border astrocyte density (GFAP/total cells) in comparison to AAV6-GFP control (18.86% \pm 2.56; n = 3) at 56 dpi (Fig. Sf). Interestingly, LV-Gsxl-GFP did not significantly reduce reactive gliosis $(27.77\% \pm 3.53; n = 3)$ at 14 dpi (Fig. Sb), CSPGs $(1.91\% \pm 0.19; n = 3)$ (Fig. 5d) and astrocyte density (10.18% \pm 0.49;n = 3) (Fig. Sf) at 56 dpi compared with the AAV6-GFP control, howeverdisplayed a trend toward glial scar reduction. These results suggest that AAV6-Gsxl reduced astrocyte populations during reactive gliosis and scar border maturation. Thus, our Gsxl-transduced NSPCs produced less glial fated cells (Fig. 5), e.g., astrocyte subtypes, and instead promoted differentiation into neuronal subtypes such as excitatory interneurons (Fig. 4).

 ${\it Gsxl\ promotes\ 5-HT\ neuronal\ activity\ and\ locomotor\ ftmctional\ recovery} in\ the\ chronic\ SCI$

The serotonergic (5-HT) neuronal activity is required for the normal transmission of signal in the spinal cord to generate autonomic, motor, and sensory function [35,36]. Locomotor function is directly impacted by 5-HT activity, by modulating spinal network activity required for motor control [37]. After SCI, a loss of 5-HT projections occurs resulting in innervation of motoneurons [37-39]. Thus, the restoration of 5-HT neuronal activity is necessary to promote effective signal transmission through motor circuits in the injured spinal cordand facilitate locomotor recovery. To examine this, we performed IHC to examine 5-HT neuronal activity at 56 dpi. The 5-HTsignalwasextremely
denseand distributed in parallel projections from rostral to caudal. The rostral signal was interrupted by the lesion core and did not continue into
caudal spinal cord in our control (Fig. 6a). We found that AAV6-Gsxl (6.54% \pm 0.46; n = 3) and LV-Gsxl-GFP (6.56% \pm 0.30; n =3) increased 5-HTrelative intensity

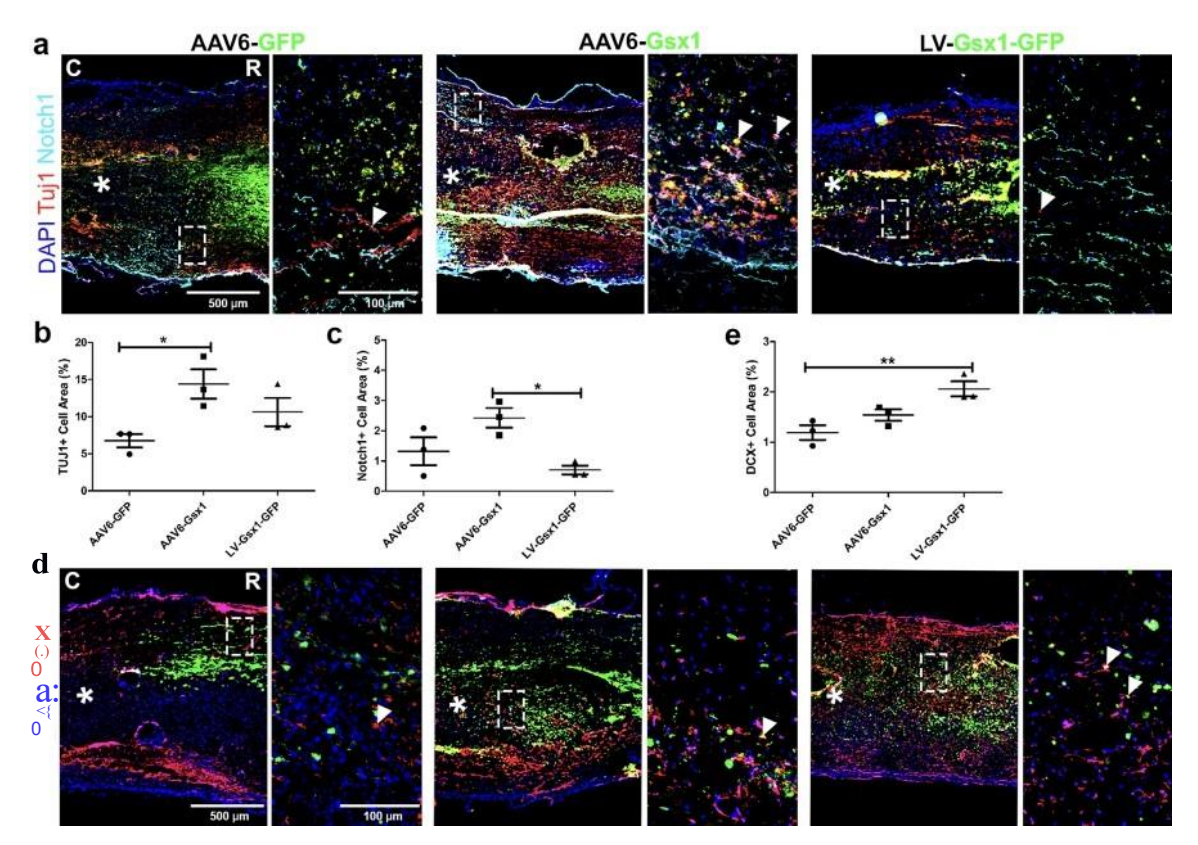


Fig. 3. Gsxl promotes neurobl andimmature neuron formation in subacute SQ. (a) Representative immunofluorescence photomicrograph of virally transduced cells (green), immature neurons (Tujl, red), and canonical notch activity (Notchl, cyan) in longitudinal spinal cord sections at 14 dpi. (b) Percent of Tujl+ cells adjacent to the lesion epicenter. (c) Percent of Notchl+ cells adjacent to the lesion epicenter. (d) Representative immunofluorescence photomicrograph of virally transduced cells (green) and neuroblasts (DC) {, red) in longitudinal spinal cord sections at 14 dpi. (e) Percent of ocx+ cellsadjacent to the lesion epicenter. Data are expressed as mean \pm SEM. *p < 0.05, **p < 0.01, AAV6-Gsxl and LV-Gsxl-GFP versus the control group (AAV6-GFP). Statistical analysis was peiformed using a one-way ANOVA followed by Tukey's post hoc test.

in comparison to AAV6-GFP control ($4.27\% \pm 0.56$ n = 3) at 56 dpi (Fig. 6b). In our treatments, 5-Hf signal continued through the lesion core in two ways: (1) directly through the lesion core with no interruption in the AAV6-Gsxl group, (2) around the injury epicenter and penetrating through the scar border in the LV-Gsxl-GFP group (Fig. 6a). Thus, Gsxl promotes restoration of neuronal activity and sprouts neuronal circuits through the lesion core at 56 dpi.

To examine the effect of Gsxl therapy on the locomotor functional recovery in injured animals, a blinded analysis of an open field locomotor test was performed with the Basso, Beattie, Bresnahan (BBB) locomotor scoringscale assessed at 1, 14, 35, and 56 dpi. BBBscores in rats with the injection of AAV6-Gsxl (13.5 \pm 0.31 at 35 dpiand 14 \pm 0.21 at56dpi; n =12) and LV-Gsxl-GFP (14.4 \pm 0.48 at 35 dpi and 15.2 \pm 0.33 at 56 dpi; n = 10) show significantly increased functional locomotor recovery compared with the AAV-GFP control (11.95 \pm 0.44 at 35 dpi and 12.6 \pm 0.43 at 56 dpi; n = 10) (Fig. 6c and Supplemental Fig. S12).

The BBB locomotor scoringscaleis divided into three major recovery stages: early (1-7), intermediate (8-13), and late (14-21) [40,41]. At 35 dpi, Gsxl rescued coordination of injured animals. Our controls (SCI+AAV6-GFP) remained in the intermediate stage, defined by uncoordinated and inconsistent hind limp plantar stepping, and our treatment groups ascended into the late stage, defined by coordination of front and hind limbs and consistent plantar stepping. At 56 dpi, Gsxl treated animals continued to improve coordination between front and hind limbs and display consistent plantar stepping, whereas control animals still showed uncoordinated movement and inconsistent plantar stepping in the hind limbs. However, the Gsxl treatment did not restore bladder functions. Overall, the Gsxl therapy resulted in the restoration of coordinated function in the hind limbs, consistent weight bearing plantar

steppingbeginning at 5 weeks, and development of variable coordination between forelimbs and hindlimbs at 8 weeks. In contrast, complete hind limb coordination was never observed in the control animals.

Gsxl does not change endogenous neuronfun.ctinn after SCI

Neuronal degeneration, demyelination, dysfunction and death occur after SCI due to primary mechanical damage and prolonged inflammatory response in the acute and subacute SO phases [11]. Torule out any secondary effects of the Gsxl therapy and account for the established AAV6 neuronal tropism, we investigated Gsxl-mediated changes in neuron populations at 14 dpi. IHC analysis was used to examine the spinal cord for established molecular markers MAP2 or NeuN (mature neurons), Caspase-3 (cell death), 5-Hf (serotonergic neuronal activity), Myelin Basic Protein (MBP, myelination), and Synaptophysin (synapses).

Fluorescence imaging of mature neurons was conducted approximately 2 mm away from the lesion core due to high neuronal celldeath. The NeuN and MAP2 mature neuron signal wasobserved 2 mm rostral to the lesion core and not present caudal (Supplemental Figs. S13a and S13c). LV-Gsxl-GFP (10.14% \pm 1.24; n = 3) and AAV6-Gsxl (11.36% \pm 0.54; n = 3) did not increase the percentage of NeuN+ cells compared with the AAV6-GFP control (14.41% \pm 1.34; n = 3) (Supplemental

Fig. S13b). Cell counting analysis showed the percentage of GFP+ and MAP2+ co-labeled cells amongvirally infected GFP+ cells in AAV6-Gsxl (84.33% \pm 0.25; n = 3) and AAV-GFP groups (85.91% \pm 2.39; n = 3) were significantly greater than LV-Gsxl-GFP (67.63% \pm 1.83; n = 3) group (Supplemental Fig. S1 3e). The Caspase-3 (Casp-3) signal was concentrated around the lesion core and dispersed 1 mm rostral/caudal (Supplemental Fig. S13c). We found that AAV6-Gsxl (51.29% \pm 4.08; n

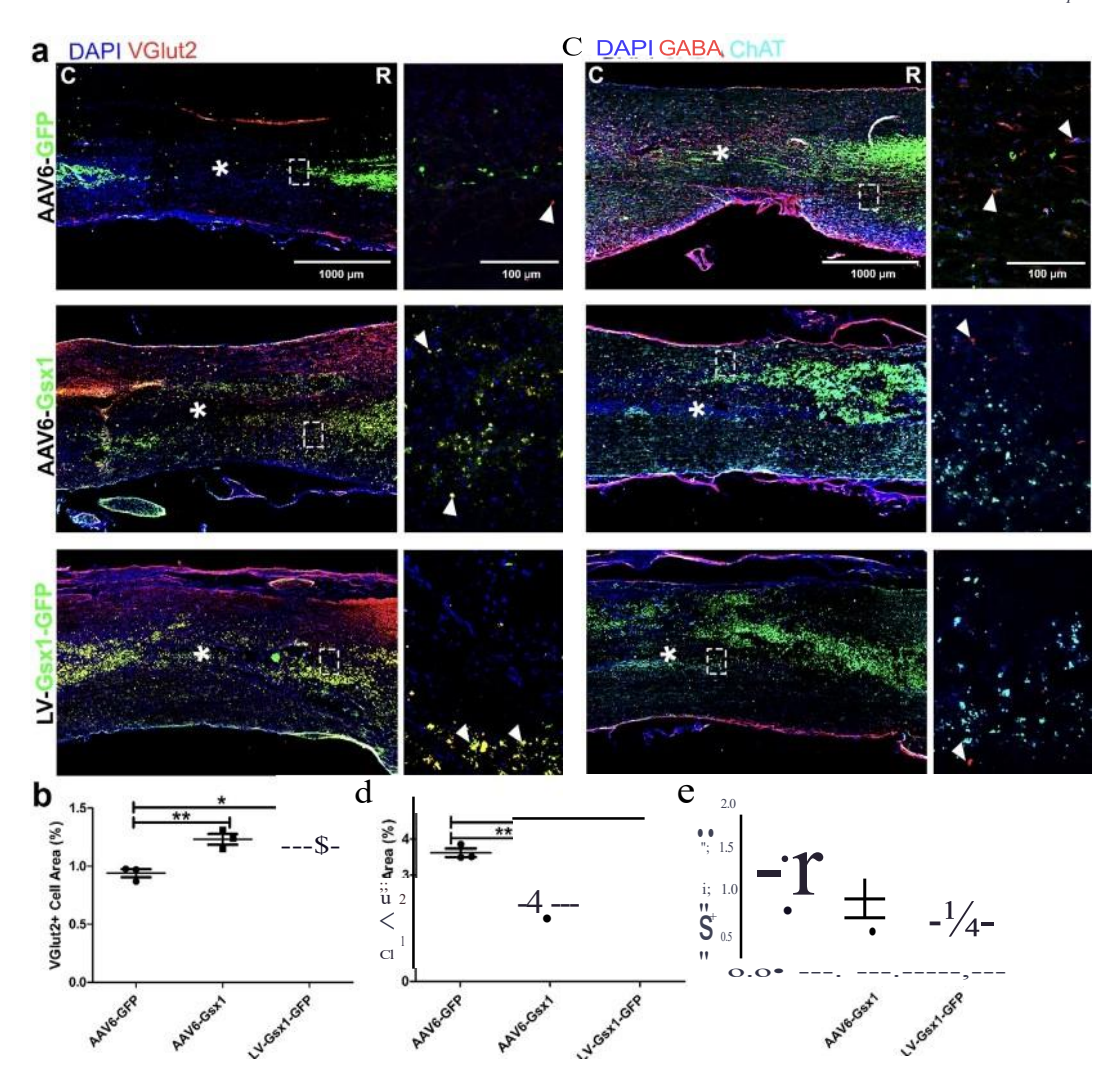


Fig. 4. Gsxl increases excitatory and redures inhibitory interneuron populations in chronic SCL (a) Representative immunofluorescence photomicrograph of virally transduced cells (green), excitatory interneurons (vGlut2, red) in longitudinal spinal cord sections at 56 dpi. (b) Percent of vGlut2+ cells adjacent to the lesion epicenter. (c) Representative inununofluorescence photomicrograph of virally transduced cells (GFP, green), inhibitory interneurons (GABA, red) and cholinergic interneurons (ChAT, cyan) in longitudinal spinal cord sections at 56 dpi. (d) Percent of GABA+ cells adjacent to the lesion epicenter. (e) Percent of ChAT+ rells adjacent to the lesion epicenter. Data are expressed as mean± SEM. *p < 0.05, ••p < 0.01, AAV6-Gsxl and LV-Gsxl-GFP versus the control group (AAV6-GFP). Statistical analysis was performed using a one-way ANOVA followed by Tukey's post hoc test.

= 3) and LV-Gsxl-GFP ($45.09\% \pm 4.15$; n = 3) did not enhance neuron survival as compared to the percentage of GFP+/Casp-3+ co-labeled cells among MAP2+ cells in AAV-GFP ($45.32\% \pm 4.92$; n = 3) control group (Supplemental Fig. Sl3d).

The MBP signal was observed rostral to and throughout the lesion core border (Supplemental Fig. S14a). AAV6-Gsxl (61.54% \pm 4.12; n = 3) and LV-Gsx:1-GFP (48.09% \pm 7.77; n = 3) did not increase neuron myelination (GFP+/MBP+ cells among MAP2+ cells) in comparison to AAV-GFP (55.58% \pm 3.28; n = 3) control (Supplemental Fig. S14b). The 5-HTsignal was distributed clearly rostral to the lesion core and was not present caudal (Supplemental Fig. S14c). AAV6-Gsxl (17.12% \pm 4.16; n = 3) and LV-Gsx:1-GFP (24.87% \pm 6.12; n = 3) do not promote serotonergic neuronal activity (GFP+/5-HT+ cells among MAP2+ cells) in comparison to AAV-GFP (21.06% \pm 6.14; n = 3) control (Supplemental Fig. Sl 4d). The Synaptophysin signal was distributed rostral and caudal to lesion core (Supplemental Fig. S14e). We also found that AAV6-Gsxl $(30.21\% \pm 1.29; n = 3)$ and LV-Gsxl-GFP $(33.98\% \pm 4.09; n = 3)$ do not promote neuronal 5Yllaptogenesis(GFP+/SYN+ cellsamong MAP2+ cells) in comparison to AAV-GFP (22.52% \pm 3.20; n = 3) control (Supplemental Fig. S140.

Overall, the Gsxl treatments infected mature neurons but did not enhance neuronal survival, serotonergic neuronal activity, myelination, or synapse formation at 14 dpi. This suggests that Gsx:1-induced functional locomotor recovery is due to neurogenesis at 4 dpi, newborn neuron formation at 14 dpi, and regeneration of neurons and neuronal activity at 56 dpi.

Discussion

Our previous study established the efficacy of LV mediated Gsxl expression to promote functional locomotor recovery in a mouse model of lateral hernisection SCI [15). In this study, we found that AAV6 infects NSPCs with highest efficiency(Fig.1). The targeting of endogenous NSPC populations prior to Gsxl efficacy testing wasan important step to move the technology forward forclinical use and maintain or increase efficacy. The LV delivery system results in robust transgene expression, however, is prone to host insertional mutagenesis [20). Here, we transitioned from the LV to a clinically safe AAV6 delivery 5Y stem [21] and demonstrated the novel application of AAV6 to target NSPCs in the injured spinal cord. We used a larger murine rat SCI model, to select for NSPC specific

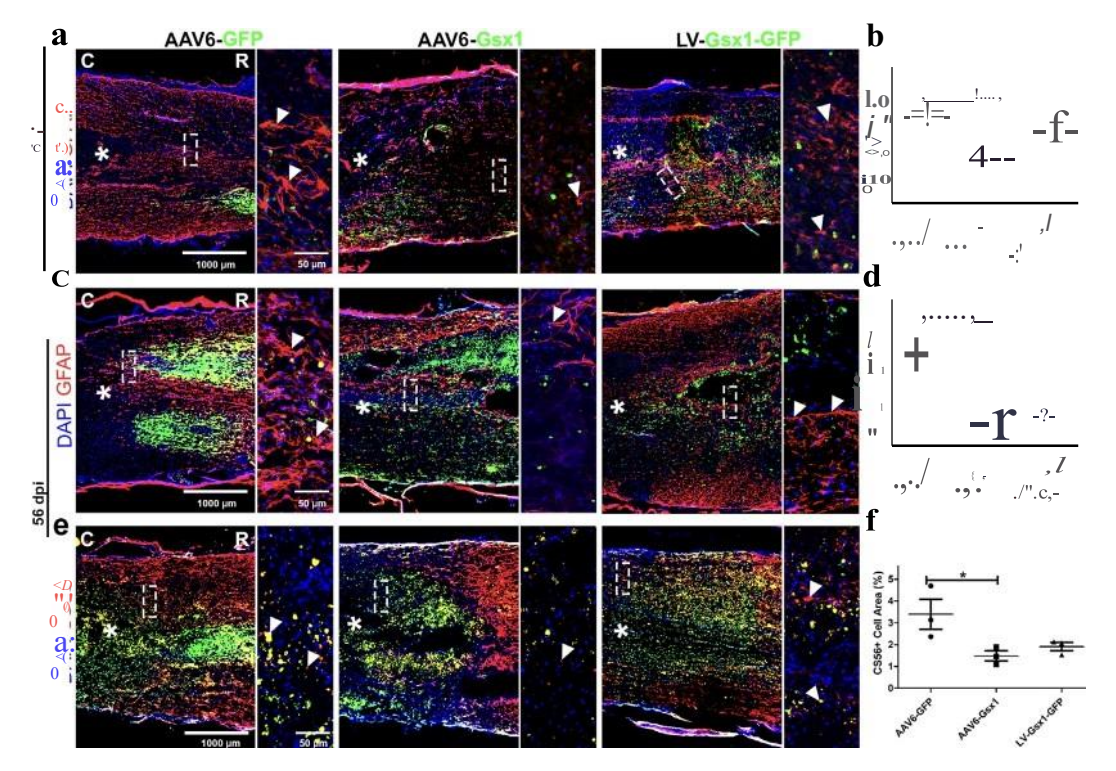


Fig. 5. Gsxl reduces reactive gliosis and glial scar formation in subarute and chronic SCI. (a) Representative immunofluorescence photomicrograph of virally transduced cells (green) and astrocytes (GFAP, red) in longitudinal spinal cord sections at 14 dpi. (b) Pen:ent of GFAP+ cells adjacent to the lesion epicenter. (c) Representative immunofluorescence photomicrographof astrocytes (GFAP, red) and gene therapy (Virus, green) in coronal spinal cord sections at 56dpi. (d) Percent of GFAP+ cells in the glial scar border adjacent to the lesion epicenter. (e) Representative immunofluorescence photomicrograph of virally transduced cells (green) and chondroitin sulfate proteoglycans (CSPG) (CS56, red) in longitudinal spinal cord sections taken at the lesion edge at 56 dpi. (f) Pen:ent of CS56+ signal in the scar border adjacent to the lesion epicenter. Data are expressed as mean± SEM. *p < 0.05, AAV6-Gsxl and LV-Gsxl-GFP versus the control group (AAV6-GFP). Statistical analysis was performed using a one-way ANOVA followed by Tukey's post hoc test.

AAVserotypes and evaluate Gsxl therapeutic efficacy. Major differences between the mouse model of SQ and human clinical SQ include increased regenerative capacity in mice [42], cystic cavity formation in humans [43], and varying inflammatory reactions [44]. However, in both the human and rat SCI pathophysiology, spontaneous regeneration does not occur and fluid filled cysticcavities form [45]. Thus, a rat model of SCI is more representative of clinical human injury and was used for all experiments.

Previously, AAV6has beenshown to target neuronal populations in the CNS, e.g., motoneurons [25], dorsal root ganglion (DRG) neurons [46,47], and many others[48]. AAV serotypes including AAVI, 2, 5, 6, 9, exhibit a known tropism for microglia and astrocytes [25,49]. Weshow AAV6 preferentially infects Nestin+ NSPCs in a rat model of acutelateralhemisection SCI. This finding provides a viable delivery system to target NSPCs in the injured spinalcord andcanbe custom.ired witha cellspecificpromotor, e.g., NG2 for polydendrocytes [50] and Foxjl for ependymal cells [51].

Most clinical SQ cases are traumatic and occur due to sports, vehicular accidents, and falls [52]. Thus, the contusion/compression SCI type is moot representative of clinical pathopiysiology [53]. Our studies demonstrated the efficacy of AAV6- and LY-mediated Gsxl delivery in both rat models oflateral hemisection and clinically relevant contusion SQ. These findings support the utility of the Gsxl therapeutic in the heterogeneous clinical setting and provide a delivery method to target NSPCs in the CNS for future therapeutic applications. We alsocompared commonly used SCI models in the field and provide insight into differences between Gsxl reactivation in distinct acute SQ types. Promising results in both SCI types serves as evidence that the Gsxl therapeutic can be used to treat heterogeneous clinical SQ, as the rat models of lateral hemisection and contusion SQ are extremely distinct and contusion injuries occur frequently in the clinic.

The AAV6 mediated Gsxl expression induces neurogenesis (Figs. 2 and 3), increases the number of neuroblasts/immature neurons (Fig. 3) and excitatory interneurons (Fig. 4), reduces inhibitory interneurons (Fig. 4) and glialscarring (Fig. 5), and restores neuronal activity (Fig. 6) in a rat model of contusion SQ. The Gsxl gene therapy significantly increases functional locomotor recovery using both the AAV6 and LV delivery system (Fig. 6). The Gsxl gene therapy results in the restoration of coordinated function in the hind limbs, consistent weight bearing plantar steppingbeginning at 5 weeks, anddevelopment of variable coordination between forelimbs and hindlimbs. This difference could signify a major change in the quality of life and independence of SQ patients.

In recent years, other neurogenic transcription factors have been used to promote functional locomotor recoveryin the injured spinal cord[54]. LV driven Sox2 expression in NG2 polydendrocytes after SQ reduced glial scar formation, promoted local network restoration, and promoted functional locomotor recovery [17]. LV driven NeuroDl expression directlyreprogrammed glial cells into functional neurons and promoted locomotor recovery [16]. A recent study identified a single recovery-organizing population of excitatory interneurons that is necessary and sufficient to regain walking after paralysis in both mice and humans [55]. Consistent with this finding, our Gsxl therapy promotes excitatory and reduces inhibitory neurons, indicating restoring excitatory/inhibitory ratiomay be required to achieve therapeuticeffects [56].

Overall, we identify an AAV serotype 6 with the highest affinity for NSPCsin the injured spinal cordand demonstrate the efficacy of the Gsxl gene therapy in a clinically relevant rat model of contusion SQ. We bring this technology one step closer to human clinical trials and demonstrate the efficacy of both LV- and AAV6- based Gsxl gene therapy to treat SQ in a rat model using clinically relevant contusion injury, and safe gene delivery method. The next stages of development for the Gsxl therapy

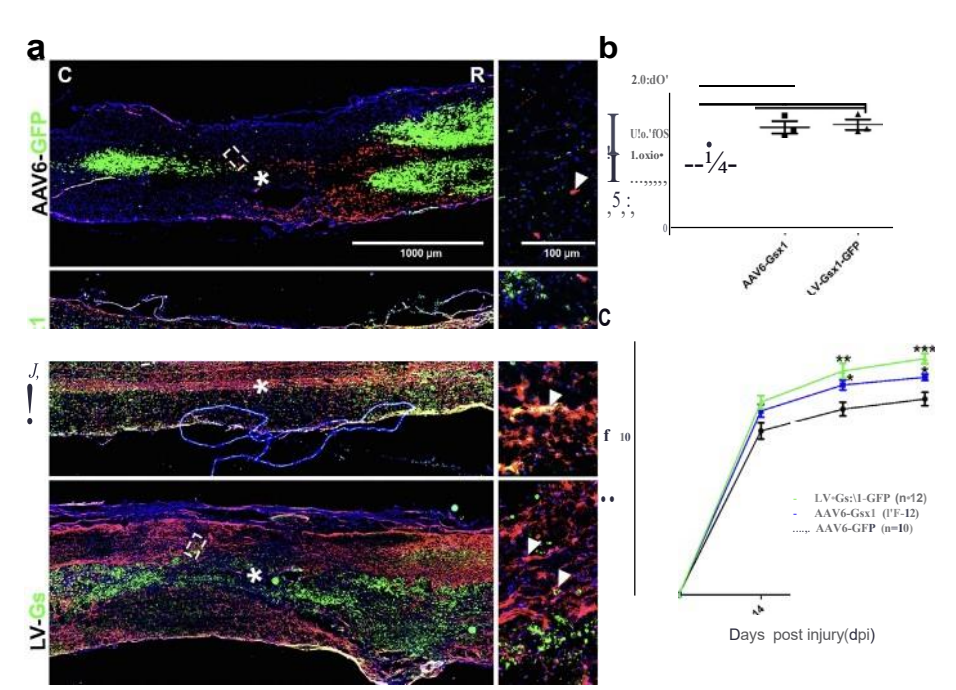


Fig. 6. Gsxl indures local network restoration and promotes functional recove,y in chronic SCI. (a) Representative immunofluorescence photomicrograph of virally transduced cells (green) and serotonergic neuronal activity (5-fIT, red) in longitudinal spinal cordsections at 56 dpi. (b) Relative Intensity of 5-HT+ cells through the lesion epicenter. (c) Impact of AAV6- and LV-mediated Gsxl treatment on functional recovery after chronic contusion SCL Data are expressed as mean \pm SEM. *p < 0.05, **p < 0.01, ***p < 0.001, AAV-Gsxl and LV-Gsxl-GFP versus the control group (AAV6-GFP). Statistical analysis was performed using a two-way repeated measures ANOVA followed by Tukey's post hoc test.

are preclinical examination in larger mammals, e.g., canine, swine, or proceed to human clinical trials. Further mechanistic understanding of Gsxl reactivation is necessary to consider *this* for treatment in humans. Limitations of the study include cell/molecular quantification techniques, i.e., IHC, which examines the protein content and distribution. Next-generation sequencing techniques, e.g., single-cell transcriptomic and ChIP-seqanalysis, maybe the nextstepto understand the mechanism of Gsxl gene therapy. It should be noted that proteinexpression dictates cellular function, therefore this study provides further understanding of Gsxl-induced changes in cellular function after SCI.

Materials and Methods

AAV and LV constructs

Viral constructs:ssAAV5-CMV--eGFP, ssAAV6-CMV--eGFP, ssAAVrhl0-CMV-eGFP, ssAAV6-CMV--eGFP, and scAAV6-CMV-Gsxl were manufactured byVectorBiolabs (Malvern, PA); LV-CMV-eGFP and LV-CMV-Gsxl-SV40-eGFP were manufactured by Applied Biological Materials Inc. (Richmond, BC, Canada).

Rat model of lateral hemisection SCI

Male Sprague Dawley rats (8-12-week-old) were purchased from Charles River Laboratories. Rats were acclimated to the animal facility for1 week. Rats wereanesthetiz.ed with 3% Isoflurane and maintaioed at 2% Isoflurane, then placed on heating pad set to low. Eye lubricant was applied, the surgical site shaved, and steriliz.ed using betadine and 70% ethanol solutions. Analgesics were administered including buprenorphine SR and bupivacaioe 0.125%. An incision was made with 10 blade scalpel between cervical and lumbar spinal level. The muscle was dissected using surgical microscissor.; and remove the dorsal process of thoracic vertebrae 9 (T9) and Tl0 were removed with bone rongeur to expose the spinal cord. A clamp was applied to the surrounding muscle and a lateral hernisection spinal cord injury was generated via surgical rnicroscissor. 1.5 μL virus treatment was injected in the BSL2 facility at 500 nL/rnin using 10 µL Hamilton syringe at 1.0 mm rostral/caudal to injury site. Avolume of 0.5 µLvirus treatment was injected at depths: 0.5 mm, 1.0 mm, 1.5 mm to ensure total 3.0 µL virus penetrates throughout the injured spinal cord. Adipose tissue from the nape of neck was

removed and placed on the exposed T9-10 spinal cordinjurysite. Two 3-0 sutures were applied to close the muscle and fat adjacent to the laminectomy. Wound clips were applied, and the animal was placed in recovery cage on heating pad and observed until awake and alert. Sterile saline was administered throughout the surgery to ensure animal hydration and cefazolin antibiotic was administered immediately after the surgery. Food and water were provided ad libitum.

Animals were monitored daily for pain, distress, hydration, and surgical site infection. Animal bladder.; expressed twice daily and administered 1.0 rnLbolus saline and cefazolin antibiotic daily for the duration of the study. Bladder infections were treated with enrofloxacin and autophagia was treated with acetaminophen as needed. All procedures were carried out under protocols approved by the Rutgers University InstitutionalAnimal Careand Use Committee and conformed to NIH guidelines. Rutger.;Institutional Animal Care and Use Committee (IACUC) Protocol 999900038.

Rat model of contusion SCI

Female Sprague Dawley rats (8-12-week-old) wereanesthetiz.ed with isoflurane (2.5%) before performing a larninectomy to remove the dorsal process of thoracic vertebrae 9 (T9) and expose the spinal cord. The lateral processes of T8 and T10 were clamped and a 200 kDyn injury was induced using the Infinite Horizon Impactor (Precision Systems & Instrumentation). Body temperature was monitored and maintained throughout the surgery using a thermo-regulated heating pad. Following injury, animals received viral treatment AAV6-GFP, AAV-Gsxl, or LV-Gsxl-GFP via stereotaxic injection into the 4 comers of injury site in the BSL2 facility. After injection, muscle layer.; were sutured (Ethicon) and skin was closed using wound clips and analgesics, ringer lactate, antibiotics were administered, and returned to the hazard room facility for postoperative care. Animals were housed in temperature-controlled incubator.; until normothermic and then placed in cages on temperature regulated heating pads in a recovery area. Animals were housed in pair.; in standard plastic cages. Food and water wereprovided ad libiturn. Buprenorphine (0.05 mg/kg) was administered twice-a-day for the first three days post-surgery to alleviate paio. Lactated Ringer's solution (10 ml) was provided 1-2 times per day for the fir..t three days post-surgery to prevent dehydration. Gentamycin (5 mg/kg) was administered once daily for the first 7 days post-surgery to prevent infections.

Contusion surgeries, animal care, locomotor and bladder function analysis, and euthanasia were performed by the Burke Neurological Institute at Weill Cornell Medicine (White Plains, NY). All procedures were carried out under protocols approved by the Weill Cornell Medicine Institutional Animal Care and Use Committee and conformed to NIH guidelines.

Locomotor and bladder fimction analysis

Recovery of motor function was assessed via BBB locomotor scale method [40]. Prior to recording baseline measurements, rats were allowed to adapt to the open field and pretrained for 10 days. Pre-injury baseline values were collected on the day before SQ surgery (day 0). Following SCI and gene therapy intervention rats' ability tolocomote was observed, scored, and documented on post-injury days 1, 4, 14, 35 and 56. Briefly, animals were placed on a flatsurface with 6+ inch high walls and allowed to move/walk around the "pool" for 4 min. Sham and SCI rat's joint movement, hindlimb movements, stepping, forelimb and hindlimb coordination, trunk position andstability, paw placement and tail position were monitored and scored. The scale (0-21) represents sequential recovery stages. Bladders were expressed twice daily and relative volume was measured manually.

Tissue processing, sectioning, and immlDlohistochemistry (IHC)

Animals wereanesthetized with 3% isofluraneand placedon dissection tray. An incision was made in the mid-abdomen and the diaphragm dissected. Incisions oneithersideof theribcage weremadeand theribcage pinned above the chest The heart was held with forceps and the right anterior vena cava cut using surgical microsclssor... Asafety blood collection needle was placed into the left ventricle and 15 ml standard IX Phosphate Buffered Saline(lxPBS) was pumped at a rate of 4 ml/min into the leftventricle, followed by 15 ml 4% Paraformaldehyde (PFA)solution. Vertebral columns were removed, placed on ice in 4% PFA, and animal carcasses were disposed. An 8 mmsection centered at T9-10 was dissected immediately using forceps, surgical microscissors, and bone rongeur. Rats were perfused withsaline and fixed with 4% paraformaldehyde and spinal cordswerecollected, dissected, and cryopreserved in 300/4 sucrosesolution.

Tissues were washed overnight in 4% PFA, then washed in lxPBS for 1.5 hand placed in sucrose. After 2+48 h, tissues were saturated and submerged in optimal cutting temperature (OCf) fluid at -SOC. Tissues were sectioned using cryomicrotome, e.g., coronal, or sagittal plane, at 12 μm thickness onto charged glassslidesand split into 6 major sections of the spinal cord. Sectioned tissueswerestored in long term at -80 °C or short term in 4 °C.

Cryosectioned tissueswere removed fr001-80 °C and placed in room temperature for 30 min. Tissues were rehydrated with lxPhosphate buffered saline (PBS) and placed intoslide chamber. Methanol antigen retrieval was performed for 10 min and washed with lxPBS twice for 5 min. Tissues were incubated with diluted primary antibody solutions (Supplemental Table SI) and placed overnight at 4 °C. Tissues were washed in lxPBS three times for 10 min and incubated with diluted secondary antibody solutions for 60 min at room temperature. The tissues were then washed with lxPBS twice for 10 min and incubated with diluted DAPI nuclear stain solution for 5 min. Tissues were washed in lxPBS three times for 5 min. Slides were removed from chamber and left to dry, then mounting media and glass coverslip were applied. The Gsxl antibody was used to evaluate virally infected cells in the SCI+AAV-Gsxl, as the virus is self-complementary and limited in size. Virus mediated Gsxl expression was validated by IHC using anti-Gsxl antibody (Sigma-Aldrich #SAB2104632; supplemental Fig. S15).

Microscopy and image analysis

Four to six sections from each animal were analyzed. Images were captured at the same exposure, threshold, and intensity per condition

using Zeiss AxioVision imager Al (Zeiss, Germany) and Echo Revolve (San Diego, CA) at wavelengths 488, 547, 649 nm. Images were processed and cell counted usingImageJ. Co-labeled cells with viral reporter GFP and specific markers were manually counted in separate RGB channels and merged images in an area of 438 µm by 328 µm region adjacent to the injection and lesion site. Alternatively, ZVI files were converted to TIFF format using python code and TIFFfiles are analyzed using llastik's pixel classification module [30]. Pixel intensity and area are quantified, and statistical analysis is performed. A minimum of 5--10 images per animal are required to generate data using cell counting or Ilastik analysis methods. Overall, considerations include systematic/random sampling, antibody staining clearly identifying cells or proteinof interest, and calculation of total cellsignal were made. Images containing artifacts, tissue folds, and non-specific or unclear antibody binding were excluded from analysis.

Statistical analysis

GraphPad Prism 6 was used for all statistical analysis. Comparisons between two individual groups were analyzed with two-tailed students T-test (a = 0.05). Comparisons between three groups or more were analyzed with a one-way ANOVA and Tukey multiple comparisons test (a= 0.05). BBB scores and vector biodistribution were analyzed using two-way repeated-measuresANOVA (a= 0.05) with a Tukey's multiple comparisons post hoc test.

Author contributions

Z.F., S.G., and L.C. conceived the project. Z.F. and S.K. performed the animal surgeries. Z.F., F.E, and B.R. conducted animal perfusions, tissue dissections, processing and cryosectioning. Z.F., F.E., T.C, and A.J. performed IHC. Z.F., F.E., A.J., T.C., and J.G. conducted fluorescence imaging. A.J., B.R., H.A., M.D., M.E., A.J.G., J.S., H.P., S.K.G., H.T., S.Z., S.N., performed cell counting for molecular markers. Z.F., M.J.T., and A.J.G. developed the image processing pipeline. Z.F. and F.E. analyzed IHC data. Z.F. and L.C. wrote and edited this paper.

Data availability

Alldatasupporting the results reported in the article can be found in supplemental materials including all prism files and excel files for individual data points.

Declaration of competing interest

L.C. is listed as a co-inventor in the patent application related to this work. LC. is a founderofNeuroNovus Therapeutics Inc.and a member of the scientific advisory board. S.G. was the CEO of NeuroNovus Therapeutics Inc. The remaining authors declare no competing interests.

Acknowledgments

This research was funded by the New Jersey Commission on Spinal Cord Research (NJCSCR)I5IRG006 (LC.), the TechAdvance Fund (LC.), HealthAdvance Fund (L.C.), the NJCSCR graduate fellowship 22FEL016 (Z.F.), the NIH Biotechnology Pre-Doctoral Training Fellowship T32GM008339 (T.C. and B.R.); and NSF-EEC-1950509, REU Site in Cellular Bioengineering (J.G.). M.J.T. and A.J.G. acknowledge support from NIH NIGMS R35GM138296.

Appendix A. Supplementary data

Supplementary data to this article can be found online at https://doi.org/10.1016/j.neurot.2024.e00362.

References

- [I) Sel<hon LH, Fehlings MG. f.pidemiology,demographics, and pathophyslology of acute spinal cord injury. Spine 2001;26(24 Suppl):S2 12.
- [2] LIE, Yan R, Yan K, Zhang R, Zhang Q, Zou P, et al. Single-cell RNA sequencing rewals the role of Immune-related autophagy in spinal cord i.njury in rats. Front Immunol 2022;13:987344.
- (3) Shi Z. Yuan S, Shi L, U J, Ning G, Kong X, et al Progn1mmed cell death m spinal cord injury pathogenesis and therapy. Cel Prolif2021;54(3):e12992.
- (4) Xu W, Chi L, Xu R, Ke Y, LuoC, ca; J, et al. Itxreased production of reactive oxygen species contributes to motor neuron death in a compression mouse model of spinal cord Injury. Spinal C.Ord 2005;43(4):204-13.
- (5] Park E, Velumian AA, Fehlings MG. The role of excitotoxlcity in secondary mechanisms of spinal cord injury:a review w;th an emphasis on theimplications for white matter degeneration. J Neurocrauma 2004;21(6):754 7 ◄.
- (6) Molofsky AV, Parda! R, Iwashita T, Park IK, Oarke MF, Morrison SJ. Bml-1 dependence distinguishes neural stem cell self-renewal from progenitor proliferation. Nature 2003;425(6961):962-7.
- [7] Finkel Z, Esteban F, Rodriguez B, Fu T, Ai X, Cai L. Diversity of adult neural stem and projlellitor cells In physiology and disease. Cells 2021;10(8).
- (8) Maichal N, Reali C, Tntjillo-Cenoz 0, Russo RE. Spinal cord stem cells in their microenvironment: the ependyma as a stem cell niche. Adv Exp Med Biol 2017; 1041:55-79.
- [9] Bond AM, Berg DA, Lee S, Garda-Epelboim As, Adusumilli VS, Ming GL, et al. Differential timingand coordination of neurogenesis and astrogenesis in dew loping mouse hippoc:ampal subregions. Brain Sci 2020;10(12).
- [10] Hesp ZC, Yoseph RY, Suzulci R, Jukkola P, Wtlson C, Nlsluyama A, et al. Proliferating NG2-cell-dependent angiogenesis and scar fonnation alter axon growth and functional recovery after spinal cord injury in mice. J Neurosd 2018; 38(6):1366-82.
- (11] Clifford T, Finkel Z, Rodriguez B, Joseph A, Cai L. Current advancements in spinal cord injury research-glial scar formation and neural regeneration. Cells 2023;12(6).
- (12] Chapman H, Riesenberg A, Ehrman LA, Kohli V, Nardini D, Nakafuku M, et al. Gsr transcription factors control neuronal versus glial specification in ventricular zone progenitors of the mouse lateral ganglionic eminence. Dev Biol 2018;442(1): 115–26
- (13] Pel Z, Wang B, aienG, Nagao M, Nakafuku M, Campbell K. Homeobox genes Gsxl and Gsx2 differentially regulate telencephalic progenitor maturation. Proc Nati Acad Sci USA 2011;108 (◄):1675-80.
- (14] Gupta S, Kawaguchi R, Heinrichs E, Gallardo S, Castellanos S, Mandric I, et al. In vitro atlas of dorsal spinal interneurons reveals WntsignaUng as a critical regulator of progeniror expansion. Cell Rep2022;40(3):111119.
- (15) Patel M, LIY, Anderson J, castro-PedridoS, Skinner R. LeiS, et al. Gsxl promotes locomotor flDlctional recovery after spinal cord injury. Mol Ther 2021;29(8):
- (16) Su Z. NiuW,Liu Ml, ZOu Y,ZhangO.. In vivoconversionofastrocytesto neuronsin the Injured adult spinal cord Nat C.Ommun 2014;5:3338.
- (17] Tai W, Wu W, Wang LL, Ni H, Chen C, Yang J, et al. In vivo reprogramming of NG2 glia enables adult neurogenesis and functional recovery following spinal cord injury. CellStem Cell 2021;28(5):923-937 e4.
- [18] Chen W, Zhang B, Xu S, Lin R, Wang W. Lentivirus canyling the NeuroDI gene promotes the conversion from glial cells intoneurons in a spinal cord injury model. Brain Res Bull 2017;135:143–8.
- (19] Patel M, Anderson J, LeiS, Finkel Z, Rodriguez B, Esteban F, et al. Nloc6.1 enhances neural stem cell activation and attenuates glial scar fonnadon and neuroinflammation in the adult injured spinal cord. Exp Neurol 2021;345:113826.
- (20] Rarttaru M. Cesana D, Bartholomae CC. Sanvito F, Pala M, Benedicentl F, et al. Lent, viral vector-based insertional mutagenesis identifies genes associated with livercancer. Nat Methods 2013;10(2):155-61.
- (21] Naso MF, Tomkowicz B, Perry3rd WL, Strohl WR. Adeno-associated virus (AAV) as a vector for gene therapy. BioDru 2017;31(4):317-34.
- (22] RotheM, Modlich U, Schambach A. Biosafety challenges for use of lentiviral veCU>rs in gene therapy. Qn-r Gene Ther 2013;13(6):4 8.
- (23) Milone MC, Ol)oherty U. Clinical use of lentiviral vector,. Leukemia 2018;32(7): 1529-41.
- (24) Connolly JB. Lentiviruscs in gene therapy clinical research. GeneTher 2002;9(24): 1730-4.
- (25] Snyder BR, GraySJ, Quach ET, Huang JW, LelDlg OI, Samulski RJ, et al. Comparison of adeno-associated viral vector serotypes for spinal cord and motor neuron gene delivery. Hum Gene Ther 2011;22(9):1129-35.
- (26] PengSP, Kugler S, Ma 2l<, Shen YQ, Schachner M. Comparison of M V2 and AAV5 in gene transfer in the Injuredspinal cordof mice. Neurorepon 2011;22(12):565-9.
- (27) DIrren E, Towne CL, Sctola V, Redmond Jr DE, Schnelder BL, Aebischer P. Intracerebroventricular injection of adeno-assodated virus 6 and 9 vectors for cell type-specific transgene expression in the spinal cord. Hum Gene Ther 201 ◀:25(2): 100, 20

- (28] Hoshino Y, Nlshide K, Nagoshl N,Shibata S, Morltoki N, Kojima K,et al. The adenoassociated virus rh!O vector Isan effective gene transfer system for chronic spinal cord injury. Sci Rep2019;9(1):98 ◀ ◀.
- (29] Bey K, Deniaud J, Duhreil L, Joussemet B, Cristiru J, Gronc, et al. Intra-CSF AAV9 andAAVrhl0 administrationIn nonhuman primates: promising routes and vectors for which neurological diseases? Mol Ther Methods Clin Dev 2020;17:771--84.
- (30] BergS, Kutra D, KroegerT, StraehleCN, Kausler BX, HauboldC, et al. ilasli.k: interactive machine learningfa (bio)image analysis. Nat Methods 2019;16(12):1226-32
- (31] Mazzone GL, Mohammadshiratl A, AquinoJB, N"astri A, Taccola G. GABAergic mechanisms can redress the tilted balance between excitation and inhibition in damaged spinal networks. Mol Neurobiol 2021;58(8):3769 6.
- (32] Mizuguchi R. KriksS, Cordes R, Gossler A, Ma Q, Goulding M. Ascll and Gshl/2 control inhibitory and excitatory cell fate in spinal sensory intemeurons. Nat Neurosd 2006;9(6):770.
- (33] McKeon RJ, Schreiber RC, Rudge JS, Silver J. Reduction of neurite ouigrowth in a model of glial scarring ronow;ng CNS injury Is correlated with the expression of inhibitory molecules on reactiw astrocytes. J Neurosd 1991;11(11):3398-411.
- (34] Barnabe-Helder F, Goritz C, Sabelstrom H, Takebayashi H, Pfrieger FW, Meletis K, ct al. Origin of newglialcells in intact and injured adultspinalcord. Cell Stem Cell 2010;7(4):470-82.
- (35] F1aive A, Fougere M, van der 7.ouwen a, Ryczko D. Serollloergic modulation of locomotor activity from basal vertebrates to mammals. Front Neural Circ 2020;1 ◀: 590299.
- [36] Sizemore TR, Hurley LM, DacksAM. Serotonergle modulation acrosssensory modalities. J Neurophysiol 2020;123(6):2406-25.
- (37] Huang CX, Zhao Y, Mao J, Wang Z, Xu L, aieng J, et al. An injury-induced serotnnergle neuron subpopulation contributes to uon regrowth and function restoration after spinal cord injury in zei>rafish. Nat Commun 2021;12(1):7003.
- (38) Penin FE, Norisrani HN.Serotonergic mechanisms in spinalcord injury. Exp Neurol 2019;318:174--91.
- (39] Fauss GNK, Hudson KE, Grau JW. Role of descending seroronergic fibers in the development of pathophysiologyafter spinal cord injury (SCO: contribution to chronic pain, spasticity, and autonomic dysreflexia. Biology 2022;11(2).
- (◀OJ BassoDM, Beatlle MS, Bresnahan JC. Asensitiw and reliable locomotor rating scale for open field testing in rats. J Neurotrauma 1995;12(1):1-21.
- (41] Wong JK, Sharp K, Steward0. Astraight alley version of the BBB locomotor scale. Exp Neurol 2000;217(2):417 20.
- (42] Ung RV, Lapointe NP, Tremblay C, Larouche A, Guertin PA. Spontaneous recovery of hindlimb movement in completely spinal cord transected mice: a comparison of assessmE11t methods and condilions. Spinal Cord 2007;45(5):367-79.
- (43] ZhangC, Morozova AY, Abakumov MA, Gubsky n., Douglas P, FengS, et al Precise deliwry into chronic spinal cord injury syringomyelic cysts with magnetic nanoparticles MRI visualization. Med Sci Mon Int Med J ExpQin Res 2015;21: 3179 5
- (45] Kjell J, Olson L Rat models of spinal cord injury: from pathology to potential therapies. Dis Model Mech 2016;9(10):1125--37.
- [46] Buss N, Lanigan L, Zeller J, Cissell D, Metea M, Adams E, et al. Chara < 1 erization of AAV-mediated dorsal rootganglion opathy. Mo! Ther Methods ain Dev 2022;24:342-54.</p>
- (47] Kudo M. Wupuc, S. Fujiwara M,Sairo Y, Kubota S, Inoue KI. et al. Specific gene expression in IDImyelinated dorsal root ganglion neurons in nonhuman primates by intra-ner injection of AAV 6 vector. Mol Ther Method! Clin Dev 2021;23:11-22
- (48) Pellissier LP, Hoek RM, Vos RM, Aartsen WM, Kllmczak RR, HoyngSA, et al. Specific tools for targeting and expression in Muller glial cells. Mol Ther Methods ain Dev 2014;1:1 ◀OOO.
- (49] Liu G,Martins Di,Chiorini JA, Davidson BL. Adeno-as.ocialed virus type ◀(AAV ◀) targets ependyma and astrocytes in the subventricular zone and RMS. Gene Ther 2005;12(20):1503.
- (50] Nishiyama A, Komirova M, Suzuki R, Zhu X. Polydendrocytes (NG2 cells): multifunctionalcells with lineage plasticity. Nat Rev Neurosci 2000;10(1):9-22
- (SI] Mothe AJ, Tator CH. Proliferation, migration, and differentiation of endogenous ependymal region stem/progenitorcells following minimal spinal cord injury in the adult raL Neuro9Cience 2005;131(1):177-87.
- (52] Ding W,HuS, Wang P, Kang H, Peng R, Dong Y, et al. Spinalcord injury: the global incidence, prevalence, and disability from the global burden of diseasestudy 2019. Spine 2022;47(21):1532-40.
- (53) Cruu CW, aieng H, Hsieh SL.C.Ontusion spinal cord injury rat model. Bio Protoc 2017;7(12):e2337.
- [54] Finkel Z. cai L Transcription factors promo«e neural regeneration after spinal cord injury. Neural Regen Res 2022;17(11):2439-40.
- (55] Kathe C.Skinnider MA, Hutson TH, Regazzi N, Gautier M, Demesmaeker R, et al. The neurons that restore walking after paralysis. Nature 2022;611(7936):540-7.
- (56) a.en B, LIY, Yu B, Zhang Z. Brommer B, Williams PR, et al. Reactivation of dormant relay pathways in injured spinal cord by KCC2 manipulations.CeD 2018; 17

 √(3):521-535 el3.